Inhibition of proliferation and migration of hepatocellular carcinoma by knockdown of KIF3A via NF-κB signal pathway

Xuewei Zhang
Shantou University Medical College
Mingming Dong
Shantou University Medical College
Guoxing Zheng
Shantou University Medical College
Jinhao Zhu
Shantou University Medical College
Bang An
Shantou University Medical College
Zibin Zhou
Shantou University Medical College
Yonghao Bi
Shantou University Medical College
Meng Sun
Shantou University Medical College
Chuzhao Zhang
Shantou University Medical College
Junfeng Lian
Dabu People's Hospital
Shijie Tang (tangshijie1966@163.com)
Shantou University Medical College
Xinjia Wang
Shantou University Medical College
Wenjie Liu
Shantou University Medical College

Research Article

Keywords: KIF3A, Hepatocellular carcinoma, NF-κB, Proliferation, Migration

Posted Date: January 20th, 2023

DOI: https://doi.org/10.21203/rs.3.rs-2421333/v1

Abstract

Background

The up-regulation of KIF3A possibly predicts the dismal prognostic outcome of hepatocellular carcinoma (HCC). The present work is focused on investigating KIF3A's function in the growth and migration of HCC cells.

Methods

KIF3A expression and its role in predicting HCC prognosis were assessed using the TCGA and Genotype-Tissue Expression (GTEx) databases. KIF3A detection conditions in HCC patients were studied using an immunohistochemical panel. siKIF3A was created and then transfected into HepG2 HCC cells. Cell proliferation was examined with the use of the EDU and CCK8. Using the scratch wound healing assays, cell migration was assessed. RT-PCR and Western-blot (WB) assays were adopted for evaluating the expression of genes and proteins.

Results

KIF3A expression increased in HCC tissues as compared to matched non-carcinoma samples, and it was tightly associated with poor survival and risk factors (Ps < 0.05). KIF3A knockdown hindered the proliferation and migration of HCC cells (Ps < 0.05). KIF3A silencing reduced RelA (NF-κBp65) expression, thus, affecting the activity of HCC cells (Ps < 0.05).

Conclusion

In this study, the oncogene of hepatocellular carcinoma is KIF3A. Silencing KIF3A inhibited HCC cell growth and migration by suppressing the NF-κB signal pathway. KIF3A was identified as a potential new anti-HCC therapeutic target.

1. Introduction

Liver cancer (LC) refers to the third most normal factor leading to cancer-associated death globally and is characterized by a high mortality rate and aggressiveness [1]. Hepatocellular carcinoma (HCC) is a common histological subtype of LC, which originates from hepatocytes and has a high level of aggressiveness [2]. Chronic hepatitis B/C virus (HBV/HCV) infection and excessive drinking are the two main reason for HCC [3]. Furthermore, nonalcoholic fatty liver disease (NAFLD), which manifests as a metabolic syndrome, may increase the risk of LC. Cirrhosis can be caused by chronic liver disease, which promotes various epigenetic/genetic changes in HCC development [4]. Although early cases of LC may benefit from candidate treatments like surgery and liver transplantation[5], about 80% of cases are

already advanced when they are diagnosed [6]. Consequently, more researches are required with the aim of understanding the pathogenic mechanism of HCC and detecting novel candidate therapeutic targets for improving the prognosis of HCC.

A primary cilium is a rod-shaped organelle present on the surface of most mammalian cells, including embryonic cells, stem cells, and some tumor cells [7]. The primary cilium was discovered as early as the 1990s and was given that name by Sergei Sorokin in 1968[8]. The primary cilium has traditionally been considered to be evolved from the degradation of flagella without any significant function [9]. However, recent studies have identified the underlying function of primary cilia in controlling cell division and signal transduction [10]. Primary cilia, as signal receptors, can regulate and control the entire process of signal transduction in cells and have received a lot of attention in recent years. The correlation between primary cilia and cancer depends on tumor type, as well as differences within the same tumor and between tumor subtypes [11].

The characteristics of tumors include impaired apoptosis and the inability of cells to divide infinitely. The changes to normal intracellular or intercellular signaling pathways will also disrupt primary cilia-mediated signaling pathways, which will induce tumor genesis and progression[12]. Primary cilia disintegration must occur prior to mitosis and is critical in human diseases, particularly tumors. Therefore, primary cilia are yet another novel target that cannot be overlooked in tumor therapy. IFT proteins are essential for the transport of materials into and out of primary cilia, and changes in these components can result in hair loss and human diseases. KIF3A is required for intra-flagellar transport (IFT) as well as the assembly and maintenance of mammalian cilia, which has a significant impact on the generation of primary cilia [13].

As of now, an increasing number of studies indicate that KIF3A expression in various malignant tumors is strongly correlated with tumor genesis, its progression, and patient prognostic outcome[14]. Wang discovered that KIF3A interference by shRNA could inhibit G1/S phase transformation and metastasis of triple-negative breast cancer (TNBC) through inhibiting the Rb-E2F pathway. This finding may be due to the association of the Rb-E2F pathway with epithelial-mesenchymal transition[15]. Moreover, triple-negative breast cancer (TNBC) cells can become resistant to doxorubicin but not to cisplatin due to the high expression of KIF3A. According to Kim's study, the knockdown of KIF3A in non-small cell lung cancer (NSCLC) induced a variety of malignant phenotypes and suppressed stem cell-like characteristics[16]. In addition to interacting with β-arrestin to form a complex in NSCLC, KIF3A can inhibit β-arrestin interactions with axin and Dishevelled Segment Polarity Protein2 (DVL2), promoting J3catenin generation and thus breaking down the complex. The Wnt/β-catenin pathway activation was hindered because of the inability of β-catenin to enter the nucleus for activation and transcription activation of downstream signaling molecules [17].

The current study evaluated KIF3A levels in various tumor types from The Cancer Genome Atlas (TCGA) and their relationship to patient prognosis. In addition, the correlation between KIF3A levels and molecular pathways in HCC was analyzed[18]. Finally, this work investigated the impacts of KIF3A

silencing on HCC cell migration and proliferation. Moreover, the findings of the current work offer novel insights into KIF3A's role in HCC.

2. Materials And Methods

2.1. Bioinformatics analysis

KIF3A levels were determined using Genotype-tissue Expression (GTEx) pan-cancer data and TCGA data. Furthermore, the relationship between KIF3A levels and patient survival was investigated based on TCGA data on clinical survival. Following that, the R package cluster Profiler was added to KIF3A. The University of California, Santa Cruz (UCSC) Xena database (https://xenabrowser.net/datapages/) was used to collect KIF3A expression profiling data as well as clinical pan-cancer data from TCGA and GTEx. KIF3A levels were determined using TCGA-derived tumor samples, while healthy samples were acquired from the TCGA and GTEx databases. Person correlation and enrichment analyses were carried out on the TCGA-STAD dataset to explore the relationships between KIF3A mRNA and other mRNAs in HCC. Furthermore, 300 genes with a strong positive correlation to KIF3A were chosen for further enrichment analysis to determine KIF3A activity. Furthermore, in this study, R software cluster Profiler was used to conduct Gene ontology (GO) functional annotation for enriched GO terms using the following parameters: ont = all, q-value Cutoff = 0.05, and p-value Cutoff = 0.05. In addition, gene set enrichment analysis (GSEA) with the gsePathway and gseKEGG functions was performed in this study using the following parameters: nPerm = 1,000, maxGSSize = 1,000, minGSSize = 10, and p-value Cutoff = 0.05.

2.2. Immunohistochemical analysis

Ten cases of HCC in the Department of Pathology of the Second Affiliated Hospital of Chongqing Medical University from 2021 to now were collected and recorded by two senior pathologists. To obtain section samples, the lesion tissue samples were first fixed, dehydrated, transparent, wax immersed, embedded, and sectioned. KIF3A identification: The sections were created using an immunohistochemical method (EnVision two-step method). The samples were roasted, dewaxed, and treated with ethanol in a gradient from high to low. Soak for 5 min in 3%H_2O_2 solution; 3 times in phosphate buffer (PBS). Repair with citric acid buffer (pH = 6) at high temperature and pressure for 2 min after the pressure cooker is vented, then adjust to medium heat for 2 min before turning off the heat and stewing for 10 min. They were immersed in warm water (37°C) and cooled to 37°C, then rinsed three times with PBS buffer, later supplemented KIF3A primary antibody (rabbit anti-human monoclonal antibody), and stored at 4°C for 24 h. After removal, it was rinsed with PBS buffer 3 times. A secondary antibody (PV6000 universal antibody) was added and stored for 10 min. Then it was washed with PBS buffer for 3 times. DAB color development, PBS buffer cleaning to stop staining, ethanol concentration from low to high step-by-step dehydrating to dimethylbenzene, sealing, and processing.

2.3. Cell culture and transfection

The HepG2 HCC cells applied in the current work were offered by the Cell Bank of the Chinese Academy of Sciences (Shanghai, China) and cultured in RPMI1640 medium including 1% penicillin-streptomycin (PS) together with 10% fetal bovine serum (FBS) under 37°C and 5% CO_2 conditions. Cells were housed at our facility. siRNA was transfected into HepG2 cells to silence KIF3A in accordance with predetermined protocols for in-vitro research. Short hairpin RNA (Target sequence: GGGUUGACUUGUUGGCCAATT, UUGGCCAACAAGUCAACCCTT, GCAACUUCGCAGAGAACUUTT, and AAGUUCUCUGCGAAGUUGCTT) was acquired from Gemma Gene to manipulate the gene functions at the miRNA, RNAi, miRNA sponges, and CRISPR/Genomic Research Center, Suzhou, Jiangsu. Later, cell transfection using Lipofectamine 3000 reagent (Invitrogen) was performed in line with specific instructions. Briefly stated, cells were inoculated into a 6-well (Corning) plate and on reaching 30% density, were subjected to 48-h transfection and cultured at 37°C before being collected for qRT-PCR or subsequent analysis.

2.4. RT-PCR

In this study, the extraction of total cellular RNA was performed with the TRIzol® reagent (Invitrogen; Thermo Fisher Scientific, Inc.) following the established protocols. Fast Reverse Transcriptase (Vazyme Biotech Co., China) was used to prepare cDNA from extracted total RNA after measuring RNA content with ultraviolet analysis. The qRT-PCR assay was done by adopting TB Green Premix Ex Taq^{TM}II (With ROX) (TaKaRa biotech, China). In order to assess the heterogeneities of CT values between control and target RNA, the comparative threshold cycle (Ct) approach was applied while analyzing the results of real-time PCR. The following primers were adopted: (KIF3A, F, 5'-ATGCTTTGCTGCGTCAGTTC-3', R, 5'-ACTACTGCTGCTGCTACTGC-3'; GAPDH, F, 5'-GAGTCAACGGATTTGGTCGT-3', R, 5'-TTGATTTTGGAGGGATCTCG-3').

2.5. Western-blot (WB) assay

Cells were lysed using RIPA lysis buffer. By adopting the BCA Protein Assay kit (Beijing Solarbio Science & Technology Co., Ltd.), the protein contents were measured. Subsequently, SDS-PAGE gels were used to isolate 15–30 μg of denatured proteins, which were transferred onto a wet PVDF membrane. Later, the membranes were blocked for 15 min at 37°C with QuickBlock™ Blocking Buffer (Shanghai Beyotime Biotechnology Co., LTD), followed by overnight incubation with primary antibodies (1:1,000, Cell Signaling Technology, USA), including KIF3A (**# 8507S**) and mouse anti-βactin (# **3700S**). This was followed by rinsing the membranes with TBST and incubation using HRP-labeled goat anti-mouse or anti-rabbit IgG antibody (1:2,000, Abcam, cat. no. ab181662) for 1 h under ambient temperature. Finally, the enhanced chemiluminescence detection kit (Thermo Fisher Scientific, Inc.) was applied with the aim of visualizing the blots.

2.6. CCK8 assay

HepG2 cells (4000/well) were inoculated and cultivated in the 96-well plates. CCK8(Cell Counting Kit-8) assay was then conducted to measure cell proliferation. The 96-well plate was inoculated with cell suspension (100 μL/well) for 24 h in an incubator for pre-culture. For a specific time period, different drug concentrations were added to the culture plate. Following that, CCK-8 solution (10 μL) was supplemented

to each well (while avoiding bubbles) and incubated for another 1–4 h. To measure the absorbance (OD) at 450 nm, a microplate reader was used .

2.7. Cell wound scratch assay

The amount of liquid required for 4×10^5 cells/well was inoculated into the 6-well plate and serum culture was then added to ensure that each well contained 2 mL of the system. The bottom of the 6-well plate was covered with cells after 24 h in the cell incubator. The triangle ruler was removed, and the cross direction was marked on an overspread 6-well plate with a 100 μL medium tip. After three rounds of washing, serum-free culture was added. Photographs were then taken at the cross point under a microscope. The photographs were taken at 0, 24, and 48 h after recording.

2.8. EDU Assay

The appropriate number of cells was cultured in 6-well plates (with cover slides if necessary). 2X EdU working solution(Shanghai Beyotime Biotechnology Co., LTD) was prepared. EdU was diluted to 1X within the 6-well plate using 20 μm 2X EdU solution that had been preheated below 37°C, and cells were incubated for another 2 h. Following EdU labeling, 1 mL of fixative was supplemented after removing the culture medium, and the cells were fixed for 15-min at ambient temperature. Then, cells were rinsed three times with 1 mL washing solution for 3–5 min per well after fixation solution was removed. After removing the washing solution, 1 mL of permeable solution was supplemented to each well and incubated at room temperature for 10–15 min. After the removal of permeable fluid, the cells in each well were rinsed 1–2 times with 1 mL washing solution for 3–5 min each time. Fluorescence detection was carried out after staining the cells.

2.9. Statistical analysis

R (version 4.0.3) was adopted for all statistical analyses. The Wilcoxon rank-sum test and the paired sample t-test were applied with the purpose of determining the statistical significance of KIF3A expression in non-paired and paired tissues, separately. To examine the relationships between clinical features and KIF3A expression, the Wilcoxon rank-sum test and logistic regression were employed. In addition, all tests were two-sided, and p-values less than 0.05 were thought to be of statistical significance.

3. Results

3.1. KIF3A Expression in HCC

First, the TCGA and GTEx databases were used to analyze KIF3A levels. The findings demonstrated that KIF3A was up-regulated in 24 tumors as compared to related healthy samples, such as ACC, BRCA, BLCA, COAD, CHOL, CESC, ESCA, GBM, HNSC, KIRP, LIHC, LGG, LUSC, LUAD, OV, READ, PRAD, PAAD, STAD, SCKM, THCA, TGCT, UCS, and UCEC (Fig. 1A). KIF3A expression in HCC samples was notably higher when

compared with that in normal liver tissues ($p < 0.001$). (Fig. 1B). Furthermore, KIF3A was found to be highly expressed in HCC tissues ($p < 0.001$). (Fig. 1C). Moreover, the ROC curve showed that KIF3A expression had good predictive power, with an AUC of 0.760 (95% confidence interval [CI] = 0.716–0.804) to distinguish HCC tissues from normal tissues (Fig. 1D, Fig. 2C).

3.2 Correlations Between KIF3A Expression and Clinicopathologic Variables

According to Table 1 and Fig. 3, high KIF3A expression was related to pathologic stage (stage IV vs. stage I, $p = 0.013$) and overall survival ($p = 0.03$). Meanwhile, the univariate logistic regression analyses revealed that there existed some clinicopathological differences between the groups with high and low KIF3A expression, such as T stage (odds ratio [OR] = 1.480 $p = 0.061$) and pathologic stage (Stage III & Stage IV vs. Stage I & Stage II) (odds ratio [OR] = 1.880, $p = 0.012$). (Table 2).

Table 1
Clinicopathological differences between groups with high and low KIF3A expression.

Characteristic	Low expression of KIF3A	High expression of KIF3A	p
n	185	186	
Age, n (%)			0.250
<=60	82 (22.2%)	95 (25.7%)	
> 60	102 (27.6%)	91 (24.6%)	
T stage, n (%)			0.124
T1	99 (26.9%)	82 (22.3%)	
T2	46 (12.5%)	48 (13%)	
T3	31 (8.4%)	49 (13.3%)	
T4	7 (1.9%)	6 (1.6%)	
N stage, n (%)			0.623
N0	123 (48%)	129 (50.4%)	
N1	1 (0.4%)	3 (1.2%)	
M stage, n (%)			0.623
M0	135 (50%)	131 (48.5%)	
M1	3 (1.1%)	1 (0.4%)	
Pathologic stage, n (%)			0.013
Stage I	92 (26.5%)	79 (22.8%)	
Stage II	45 (13%)	41 (11.8%)	
Stage III	30 (8.6%)	55 (15.9%)	
Stage IV	4 (1.2%)	1 (0.3%)	
Race, n (%)			0.110
Asian	87 (24.2%)	71 (19.8%)	
Black or African American	6 (1.7%)	11 (3.1%)	
White	84 (23.4%)	100 (27.9%)	
Histologic grade, n (%)			0.207
G1	33 (9%)	22 (6%)	
G2	92 (25.1%)	85 (23.2%)	

Characteristic	Low expression of KIF3A	High expression of KIF3A	p
G3	53 (14.5%)	69 (18.9%)	
G4	6 (1.6%)	6 (1.6%)	
OS event, n (%)			0.111
Alive	128 (34.5%)	113 (30.5%)	
Dead	57 (15.4%)	73 (19.7%)	
DSS event, n (%)			0.080
Alive	149 (41%)	135 (37.2%)	
Dead	32 (8.8%)	47 (12.9%)	
Tumor status, n (%)			0.039
Tumor free	110 (31.2%)	91 (25.9%)	
With tumor	65 (18.5%)	86 (24.4%)	
Vascular invasion, n (%)			0.233
No	118 (37.5%)	88 (27.9%)	
Yes	54 (17.1%)	55 (17.5%)	
Age, median (IQR)	62.5 (51.75, 69)	60 (51.25, 68)	0.334

Table 2
Correlations of KIF3A expression with the clinicopathological features of patients (n = 370).

Characteristics	Total(N)	Odds Ratio(OR)	P value
T stage (T2&T3&T4 vs. T1)	368	1.480 (0.983–2.236)	0.061
N stage (N1 vs. N0)	256	2.860 (0.361–58.253)	0.366
M stage (M1 vs. M0)	270	0.344 (0.017–2.721)	0.357
Pathologic stage (Stage III&Stage IV vs. Stage I&Stage II)	347	1.880 (1.156–3.096)	0.012
Age (> 60 vs. <=60)	370	0.770 (0.511–1.158)	0.210
Race (White vs. Asian&Black or African American)	359	1.350 (0.892–2.048)	0.156
Residual tumor (R2 vs. R0&R1)	342	0.000 (NA-Inf)	0.996
Histologic grade (G3&G4 vs. G1&G2)	366	1.485 (0.969–2.283)	0.070

3.3. Correlations between KIF3A level and prognosis of HCC cases

Additionally, the association between KIF3A expression and overall survival (OS) was examined using data from the TCGA database to determine whether the KIF3A level had prognostic value. Therefore, KIF3A up-regulation predicted a poor prognosis for HCC (P = 0.005) (Fig. 4,5,6), indicating that KIF3A might play an oncogenic role in HCC.

3.4. Correlation Analysis and Enrichment

Correlation analysis was employed for investigating the relationship between KIF3A and other mRNAs in the TCGA-HCC dataset in order to investigate KIF3A functions and pathways. The R software cluster Profiler was then used in this study to examine possible pathways enriched by those 300 significant genes. According to GO analysis, KIF3A is primarily correlated with cell proliferation-related pathways including cell cycle checkpoints and DNA replication (Fig. 7). According to the findings, KIF3A activation was linked to the hyperactivation of several cancer-related pathways within HCC, particularly those regulating cell proliferation.

3.5. Special staining, immunohistochemistry, and genetic testing

Yellow or brownish yellow staining of cytoplasm or cell membrane indicates positive expression of KIF3A. The proportion of positive cells is used as the basis for intensity expression: Positive cells rate < 10% were negative (-), 10% or less positive cells rate 30% or less for weakly positive (+), 31% or less positive cell rate of 60% or less is positive (+ +), the positive cell rate of 61% or higher for strong positive (+ + +)(Fig. 8).

3.6. KIF3A Silencing Suppressed Malignant Phenotypes and Pathways in Hepatocellular carcinoma Cells

KIF3A expression was silenced within HepG2 cells using two KIF3A siRNA to investigate KIF3A's biological significance in Hepatocellular carcinoma cell proliferation. KIF3A expression was significantly reduced following siRNA transfection, according to RT-PCR and WB assays (Fig. 9). After that, the CCK8 assay was used to assess cell proliferation. As a result of KIF3A silencing, HepG2 cell proliferation was remarkably suppressed. Moreover, the EDU assay revealed that KIF3A knockdown remarkably suppressed the proliferation of Hepatocellular carcinoma cells (Fig. 10). KIF3A expression analyzed through qRT-PCR following si-KIF3A transfection in HepG2 cells. Suppression of HCC cell growth and invasion by KIF3A silencing (Fig. 11). KIF3A silencing reduced RelA (NF-κBp65) expression, thus, affecting the activity of HCC cells(Fig. 12).

4. Discussion

HCC accounts for a large proportion of primary LC cases, and the 5-year survival rate is < 20%. Since there is no specific targeted drug available, LC is still refractory. The effective first-line treatments for HCC are still lenvatinib and sorafenib, which inhibit several kinases[19]. The median survival time for lenvatinib and sorafenib, respectively, is only 13.6 and 12.3 months, indicating that these therapeutic agents are only marginally effective in treating HCC cases[20]. Therefore, novel therapeutic approaches are urgently required. Further research into the pathways of HCC tumorigenesis may lead to the development of novel therapeutics. HCC has a high recurrence and heterogeneity rate. KIF3A has recently been discovered to exert the vital function in the regulation of various disorders, including cancer [21]. For instance, increased KIF3A expression in NSCLC indicates a dismal patient outcome [22]. KIF3A knockdown suppresses growth, migration, and invasion of NSCLC cells [23]. According to metabolomic research, inhibition of KIF3A restrains breast cancer (BC) cell proliferation by increasing levels of anti-tumor lipids[24], including ceramides, as well as some PPARa ligands. Therefore, KIF3A is the metabolic oncogene in BC [25]. Likewise, selective small-molecular inhibitors of KIF3A can suppress neuroblastoma cell proliferation, suggesting that KIF3A might develop into an oncoprotein[26]. However, neither the prognostic significance nor the extent of KIF3A expression in different tumors has been identified. This study used TCGA-based data mining to show that KIF3A expression increased in 24 tumors compared to non-carcinoma samples, highlighting KIF3A's role as a novel oncogene in these tumors. So, using TCGA and GTEx datasets from the UCSC Xena database, this study examined KIF3A expression as well as its prognostic significance. In contrast to healthy control samples, KIF3A expression increased in ACC, BRCA, BLCA, CHOL, COAD, CESC, ESCA, GBM, HNSC, KIRP, LIHC, LGG, LUSC, LUAD, OV, READ, PRAD, PAAD, STAD, SCKM, THCA, TGCT, UCS and UCEC samples, while it decreased in the LAML samples. TCGA database analysis suggested that KIF3A showed overexpression within LC samples compared to healthy non-carcinoma samples. The poor prognostic outcome of ACC, LUAD, LIHC, MESO, SKCM and SARC was correlated with KIF3A up-regulation, indicating that KIF3A was the biomarker used to predict tumor prognosis. According to our enrichment analysis, KIF3A is correlated with cell proliferation-related pathways such as DNA replication, cycle checkpoints, and the cell cycle. A subsequent study discovered that silencing KIF3A inhibited HepG2 LC cell proliferation. Stroma cells in the tumor microenvironment (TME), particularly immune cells, exert a vital function in modulating cancer cell malignant behavior [27–29]. They have been argued to be significant for predicting prognosis and treating cancer cases [30, 31]. The proliferation of epithelial LC is observed to be aided by tumor-associated macrophages and CD8-positive T cells [32–34]. Our findings showed that LC samples with KIF3A up-regulation had significantly higher levels of M1 macrophage and CD8-positive T-cell infiltration. Furthermore, KIF3A expression was discovered to show positive relationship to M1 macrophage and CD8-positive T cell infiltration levels, suggesting that KIF3A plays a role in tumor immunology. KIF3A may collectively have a pathogenic effect on the development of LC, which is mediated by TIICs or tumor cells. The associated mechanisms should be further explored for better diagnosis and treatment of HCC.

NF-κB exerts a vital role in regulating cell death and inflammation, which are further related to the development of liver cell injury, fibrosis, or even HCC. NF-κB has been identified as an HCC marker. Studies have shown that the nuclear transcription factor NF-κB plays a vital role and is often found in an

inactive form within the cytoplasm of almost all cells. Once activated, NF- κB can only move from the cytoplasm to the nucleus to play an important role. Additionally, the activation of NF- κB has been linked to tumor genesis and development, anti-apoptosis, and an increase in tumor cell proliferation. Advanced lung adenocarcinoma patients are more likely to develop distant metastasis, which most commonly occurs in the thoracolumbar, pelvic, and long bone diaphysis of the limbs. Adenocarcinoma foci are typically found near the lung tissue, making it easier for them to directly invade and involve the ribs and thoracic vertebrae. This may be one of the main causes of metastasis. RelA (p65), an essential NF-κB family member, can bind to p50 to form an NF-κB heterodimer for regulating gene transcription[35]. RelA possesses C-terminal transactivation domains, which can be a potential activator for the transcription of genes containing the κB sites [36]. RelA is, therefore, an important molecule that promotes HCC growth and development. The role of post-translational RelA/p65 modification in the regulation of the NF-κB pathway has gradually become clear in recent years. They regulate the NF-κB pathway in a precise and intricate manner by regulating the protein interaction, stability, and degradation of RelA [37] and have a significant effect on disease genesis and progression. The majority of research on post-translational modification of RelA focuses on the phosphorylation of RelA and associated kinases. In addition, acetylation, methylation, and other modification forms are also popular topics of discussion in this field. RelA post-translational modification is associated with whole pathway transmission, and its dysregulation is closely related to several malignant diseases, making it an important reference strategy for clinical diagnosis and treatment. p27 is a potent inhibitor of cyclin-dependent kinase that drives G1's transition to S.Since regulation of p27 has been found in many malignancies and is associated with poor prognosis, elucidation of the molecular basis of regulation of p27 expression is of great significance, not only to gain insight into the biology of p27, but also to develop new cancer treatment strategies.According to our findings, silencing KIF3A significantly reduced RelA expression and promoted p27 expression, implying that KIF3A and RelA may be potential preventative and therapeutic targets in the development of LC. Therefore, silencing KIF3A or activating the KIF3A-RelA axis may have inhibited cancer cell growth and migration. This may provide another treatment for cases of advanced HCC and enhance their prognosis. Additional pre-clinical investigations are required to identify and assay KIF3A inhibitors.

The aforementioned findings suggest that KIF3A is a potential prognostic factor with a significant impact on cancer development. Collectively, this study revealed KIF3A's impact on HCC. Although further research is essential to explore and confirm the mechanisms underlying the occurrence and development of HCC, it is speculated that KIF3A is the marker used to diagnose and treat HCC.

Declarations

Authors' contributions:

Xinjia Wang, Shijie Tang, and Wenjie Liu designed the study. Xuewei Zhang, Mingming Dong, Guoxing Zheng, Jinhao Zhu, Bang An, Zibin Zhou, Yonghao Bi, Meng Sun, and Chuzhao Zhang performed the experiments. Xuewei Zhang, and Mingming Dong explored the data and prepared the Figures. Guoxing

Zheng and Jinhao Zhu investigated and interpreted the data. Xuewei Zhang wrote the main manuscript. Xinjia Wang, Shijie Tang, and Wenjie Liu revised the manuscript and supervised the project. Moreover, all authors reviewed the manuscript.

Funding:

The present study was funded by the Guangdong Science and Technology Special Fund Mayor Project (No: 20190301–65), 2020 Li Ka Shing Foundation Cross-Disciplinary Research Grant (2020LKSFG01D)

Conflict of Interest:

All authors declared no competing interests.

References

1. Bray, F., J. Ferlay, I. Soerjomataram, R. L. Siegel, L. A. Torre, and A. Jemal, *Global cancer statistics 2018: GLOBOCAN estimates of incidence and mortality worldwide for 36 cancers in 185 countries.* CA Cancer J Clin, 2018. **68**(6): p. 394–424.
2. Llovet, J. M., S. Ricci, V. Mazzaferro, P. Hilgard, E. Gane, J. F. Blanc, A. C. de Oliveira, A. Santoro, J. L. Raoul, A. Forner, M. Schwartz, C. Porta, S. Zeuzem, L. Bolondi, T. F. Greten, P. R. Galle, J. F. Seitz, I. Borbath, D. Häussinger, T. Giannaris, M. Shan, M. Moscovici, D. Voliotis, and J. Bruix, *Sorafenib in advanced hepatocellular carcinoma.* N Engl J Med, 2008. **359**(4): p. 378–90.
3. Ercolani, G., G. L. Grazi, M. Ravaioli, M. Del Gaudio, A. Gardini, M. Cescon, G. Varotti, F. Cetta, and A. Cavallari, *Liver resection for hepatocellular carcinoma on cirrhosis: univariate and multivariate analysis of risk factors for intrahepatic recurrence.* Ann Surg, 2003. **237**(4): p. 536–43.
4. Izzo, F., F. Cremona, F. Ruffolo, R. Palaia, V. Parisi, and S. A. Curley, *Outcome of 67 patients with hepatocellular cancer detected during screening of 1125 patients with chronic hepatitis.* Ann Surg, 1998. **227**(4): p. 513–8.
5. Patel, T., *Cholangiocarcinoma–controversies and challenges.* Nat Rev Gastroenterol Hepatol, 2011. **8**(4): p. 189–200.
6. Al-Salama, Z. T., Y. Y. Syed, and L. J. Scott, *Lenvatinib: A Review in Hepatocellular Carcinoma.* Drugs, 2019. **79**(6): p. 665–674.
7. Plotnikova, O. V., E. N. Pugacheva, and E. A. Golemis, *Primary cilia and the cell cycle.* Methods Cell Biol, 2009. **94**: p. 137–60.
8. Hua, K. and R. J. Ferland, *Primary cilia proteins: ciliary and extraciliary sites and functions.* Cell Mol Life Sci, 2018. **75**(9): p. 1521–1540.
9. Pala, R., N. Alomari, and S. M. Nauli, *Primary Cilium-Dependent Signaling Mechanisms.* Int J Mol Sci, 2017. **18**(11).
10. Bangs, F. and K. V. Anderson, *Primary Cilia and Mammalian Hedgehog Signaling.* Cold Spring Harb Perspect Biol, 2017. **9**(5).

11. Jackson, P. K., *EZH2 Inactivates Primary Cilia to Activate Wnt and Drive Melanoma.* Cancer Cell, 2018. **34**(1): p. 3–5.
12. Dell, K. M., *The role of cilia in the pathogenesis of cystic kidney disease.* Current Opinion in Pediatrics, 2015. **27**(2): p. 212–218.
13. Chen, J. L., S. Li, S. Zhou, S. J. Cao, Y. Lou, H. Y. Shen, J. Yin, and G. Li, *Kinesin superfamily protein expression and its association with progression and prognosis in hepatocellular carcinoma.* Journal of Cancer Research and Therapeutics, 2017. **13**(4): p. 651–659.
14. Xiang, Y., D. Lv, T. Song, C. Niu, and Y. Wang, *Tumor suppressive role of microRNA-139–5p in bone marrow mesenchymal stem cells-derived extracellular vesicles in bladder cancer through regulation of the KIF3A/p21 axis.* Cell Death Dis, 2022. **13**(7): p. 599.
15. Wang, W., R. Zhang, X. Wang, N. Wang, J. Zhao, Z. Wei, F. Xiang, and C. Wang, *Suppression of KIF3A inhibits triple negative breast cancer growth and metastasis by repressing Rb-E2F signaling and epithelial-mesenchymal transition.* Cancer Sci, 2020. **111**(4): p. 1422–1434.
16. Li, S., G. Zhou, W. Liu, J. Ye, F. Yuan, and Z. Zhang, *Curcumol Inhibits Lung Adenocarcinoma Growth and Metastasis via Inactivation of PI3K/AKT and Wnt/-Catenin Pathway.* Oncol Res, 2021. **28**(7): p. 685–700.
17. Liu, Zun, Ryan E. Rebowe, Zemin Wang, Yingchun Li, Zehua Wang, John S. DePaolo, Jianhui Guo, Chiping Qian, and Wanguo Liu, *KIF3a Promotes Proliferation and Invasion via Wnt Signaling in Advanced Prostate Cancer.* Molecular Cancer Research, 2014. **12**(4): p. 491–503.
18. Maluccio, M. and A. Covey, *Recent progress in understanding, diagnosing, and treating hepatocellular carcinoma.* CA Cancer J Clin, 2012. **62**(6): p. 394–9.
19. Yamashita, T., M. Kudo, K. Ikeda, N. Izumi, R. Tateishi, M. Ikeda, H. Aikata, Y. Kawaguchi, Y. Wada, K. Numata, Y. Inaba, R. Kuromatsu, M. Kobayashi, T. Okusaka, T. Tamai, C. Kitamura, K. Saito, K. Haruna, K. Okita, and H. Kumada, *REFLECT-a phase 3 trial comparing efficacy and safety of lenvatinib to sorafenib for the treatment of unresectable hepatocellular carcinoma: an analysis of Japanese subset.* J Gastroenterol, 2020. **55**(1): p. 113–122.
20. Vogel, A., S. Qin, M. Kudo, Y. Su, S. Hudgens, T. Yamashita, J. H. Yoon, L. Fartoux, K. Simon, C. López, M. Sung, K. Mody, T. Ohtsuka, T. Tamai, L. Bennett, G. Meier, and V. Breder, *Lenvatinib versus sorafenib for first-line treatment of unresectable hepatocellular carcinoma: patient-reported outcomes from a randomised, open-label, non-inferiority, phase 3 trial.* Lancet Gastroenterol Hepatol, 2021. **6**(8): p. 649–658.
21. Miki, H., Y. Okada, and N. Hirokawa, *Analysis of the kinesin superfamily: insights into structure and function.* Trends Cell Biol, 2005. **15**(9): p. 467–76.
22. Kim, Minsuh, Yong-Ah Suh, Ju-hee Oh, Bo Ra Lee, Joon Kim, and Se Jin Jang, *The role of KIF3A in the suppression of canonical Wnt signaling through the KIF3A and beta-arrestin complex, independent of the ciliary mechanism, in non-small cell lung cancer (NSCLC).* Cancer Research, 2016. **76**.

23. Kim, Minsuh, Young-Ah Suh, Ju-Hee Oh, Bo Ra Lee, Joon Kim, and Se Jin Jang, *KIF3A binds to beta-arrestin for suppressing Wnt/beta-catenin signalling independently of primary cilia in lung cancer.* Scientific Reports, 2016. **6**.
24. Hassounah, Nadia B., Martha Nunez, Colleen Fordyce, Denise Roe, Ray Nagle, Thomas Bunch, and Kimberly M. McDermott, *Inhibition of Ciliogenesis Promotes Hedgehog Signaling, Tumorigenesis, and Metastasis in Breast Cancer.* Molecular Cancer Research, 2017. **15**(10): p. 1421–1430.
25. Legare, Stephanie, Catherine Chabot, and Mark Basik, *SPEN, a new player in primary cilia formation and cell migration in breast cancer.* Breast Cancer Research, 2017. **19**.
26. Han, Young-Goo, Hong Joo Kim, Andrzej A. Dlugosz, David W. Ellison, Richard J. Gilbertson, and Arturo Alvarez-Buylla, *Dual and opposing roles of primary cilia in medulloblastoma development.* Nature Medicine, 2009. **15**(9): p. 1062-U114.
27. Buriolla, Silvia, Giacomo Pelizzari, Carla Corvaja, Martina Alberti, Giada Targato, Martina Bortolot, Sara Torresan, Francesco Cortiula, Gianpiero Fasola, and Alessandro Follador, *Immunotherapy in NSCLC Patients with Brain Metastases.* International Journal of Molecular Sciences, 2022. **23**(13).
28. Sahin Ozkan, Hulya, Mustafa Umit Ugurlu, Perran Fulden Yumuk, and Handan Kaya, *Prognostic Role of Immune Markers in Triple Negative Breast Carcinoma.* Pathology & Oncology Research, 2020. **26**(4): p. 2733–2745.
29. Binnewies, Mikhail, Edward W. Roberts, Kelly Kersten, Vincent Chan, Douglas F. Fearon, Miriam Merad, Lisa M. Coussens, Dmitry I. Gabrilovich, Suzanne Ostrand-Rosenberg, Catherine C. Hedrick, Robert H. Vonderheide, Mikael J. Pittet, Rakesh K. Jain, Weiping Zou, T. Kevin Howcroft, Elisa C. Woodhouse, Robert A. Weinberg, and Matthew F. Krummel, *Understanding the tumor immune microenvironment (TIME) for effective therapy.* Nature Medicine, 2018. **24**(5): p. 541–550.
30. Li, Chunxiao, Ping Jiang, Shuhua Wei, Xiaofei Xu, and Junjie Wang, *Regulatory T cells in tumor microenvironment: new mechanisms, potential therapeutic strategies and future prospects.* Molecular Cancer, 2020. **19**(1).
31. Erin, Nuray, Jelena Grahovac, Anamaria Brozovic, and Thomas Efferth, *Tumor microenvironment and epithelial mesenchymal transition as targets to overcome tumor multidrug resistance.* Drug Resistance Updates, 2020. **53**.
32. Zhang, Hongyu, Ruochen Li, Yifan Cao, Yun Gu, Chao Lin, Xin Liu, Kunpeng Lv, Xudong He, Hanji Fang, Kaifeng Jin, Yuchao Fei, Yifan Chen, Jieti Wang, Hao Liu, He Li, Heng Zhang, Hongyong He, and Weijuan Zhang, *Poor Clinical Outcomes and Immunoevasive Contexture in Intratumoral IL-10-Producing Macrophages Enriched Gastric Cancer Patients.* Annals of Surgery, 2022. **275**(4): p. E626-E635.
33. Liu, Qing, Chaogang Yang, Shuyi Wang, Dongdong Shi, Chen Wei, Jialin Song, Xiaobin Lin, Rongzhang Dou, Jian Bai, Zhenxian Xiang, Sihao Huang, Keshu Liu, and Bin Xiong, *Wnt5a-induced M2 polarization of tumor-associated macrophages via IL-10 promotes colorectal cancer progression.* Cell Communication and Signaling, 2020. **18**(1).

34. *Corrigendum to Tumor-associated macrophages regulate gastric cancer cell invasion and metastasis through TGFβ2/NF-κB/Kindlin-2 axis.* Chin J Cancer Res, 2022. **34**(1): p. 66.
35. , Hwa-Jung Kim, Eun-Kyeong Jo, , , , and *Mycobacterial Heparin-binding Hemagglutinin Antigen Activates Inflammatory Responses through PI3-K/Akt, NF-κB, and MAPK Pathways.* Immune Network, 2011. **11**(2): p. 123–133.
36. Schmitz, M. L. and P. A. Baeuerle, *The p65 subunit is responsible for the strong transcription activating potential of NF-kappa B.* Embo j, 1991. **10**(12): p. 3805–17.
37. Hu, H. Y., K. P. Li, X. J. Wang, Y. Liu, Z. G. Lu, R. H. Dong, H. B. Guo, and M. X. Zhang, *Set9, NF-κB, and microRNA-21 mediate berberine-induced apoptosis of human multiple myeloma cells.* Acta Pharmacol Sin, 2013. **34**(1): p. 157–66.

Figures

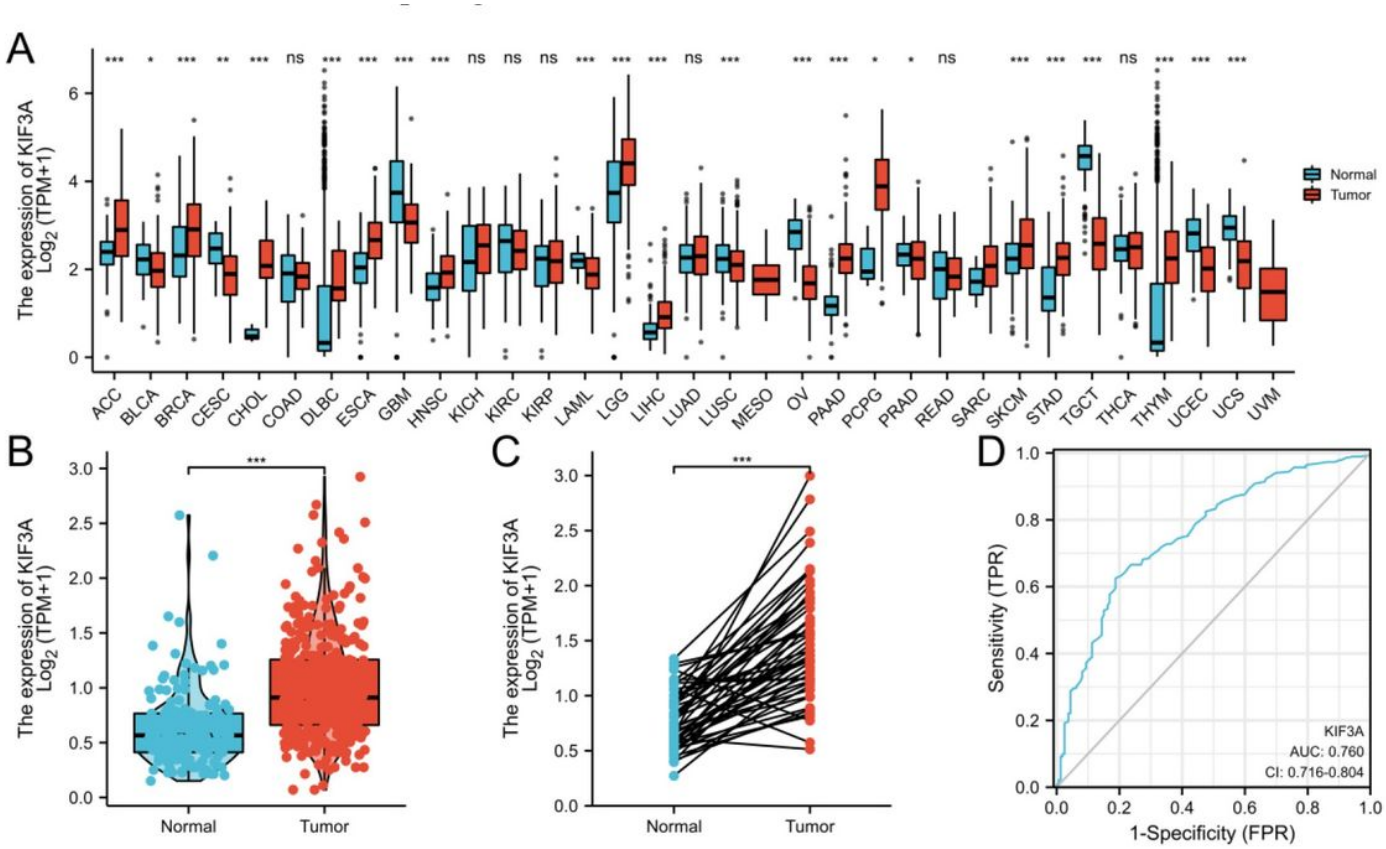

Figure 1

Levels of KIF3A in various kinds of tumors and HCC. A) Pan-cancer data from TCGA and GTEx databases showing KIF3A levels in tumor samples and corresponding non-carcinoma samples. (B) KIF3A levels in tumor samples and non-carcinoma samples from the TCGA-STAD. (C) KIF3A levels in tumor samples and matched normal tissues within TCGA-STAD. (D) ROC curves for categorizing HCC versus normal liver

tissues in the TCGA database. Moreover, the findings are shown to be mean±SD. *p<0.05, **p<0.01, ***p<0.001, ****p<0.0001.

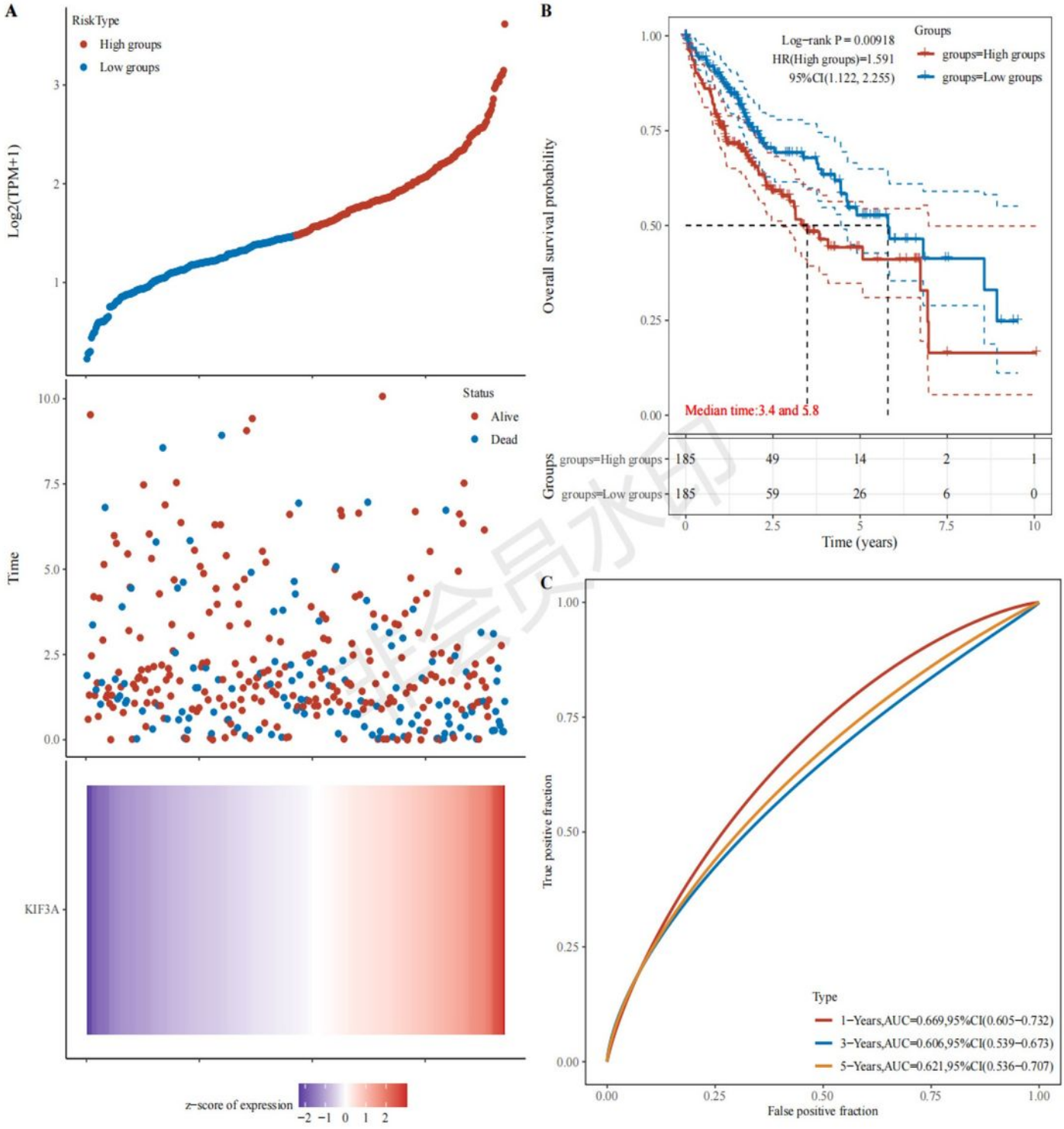

Figure 2

The gene expression, survival time, as well as survival status of the TCGA dataset. (A)The top scatterplot depicts gene expression levels ranging from low to high. Different colors represent various groups.

Besides, the scatter plot distribution depicts the gene expression of various samples in relation to survival time and survival status. The heatmap of gene expression is shown as the bottom penal. (B) Kaplan-Meier survival analysis of the gene signature from the TCGA dataset, with log-rank tests adopted for comparing different groups. The hazard ratio of the low-expression sample in comparison with the high-expression sample is indicated by HR(High exp). HR> 1 suggests that the gene is a risk factor, while HR< 1 suggests that the gene serves as a protective factor. With the use of the HR(95%CI), the median survival time (LT50) for each group was calculated. (C) The ROC curve of the gene. Higher AUC values are consistent with greater predictive power.

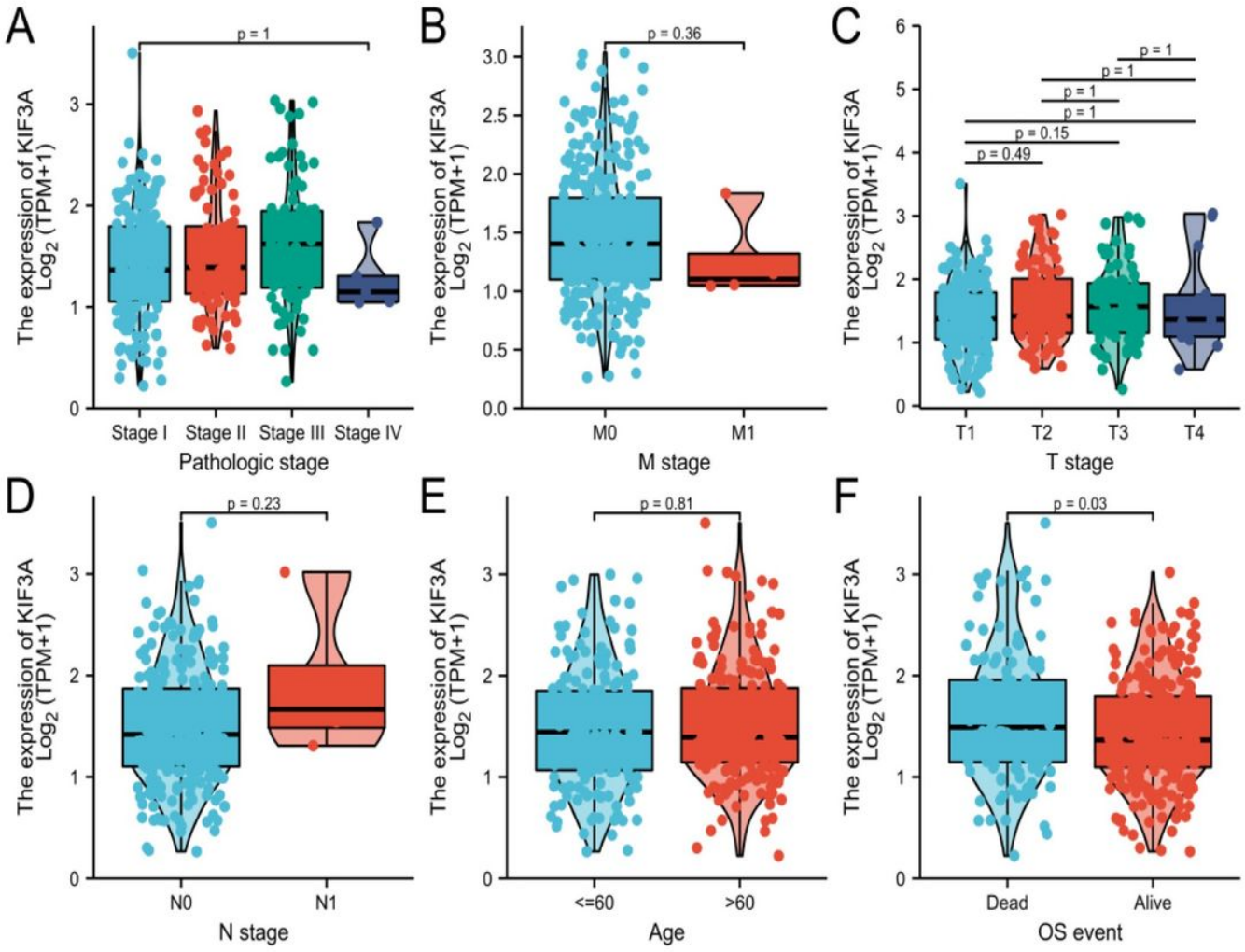

Figure 3

Correlations between KIF3A expression and clinicopathological features. In addition, data are represented for (A) pathological stage; (B)M stage; (C) T stage; (D) N stage; (E) age; (F) OS event.

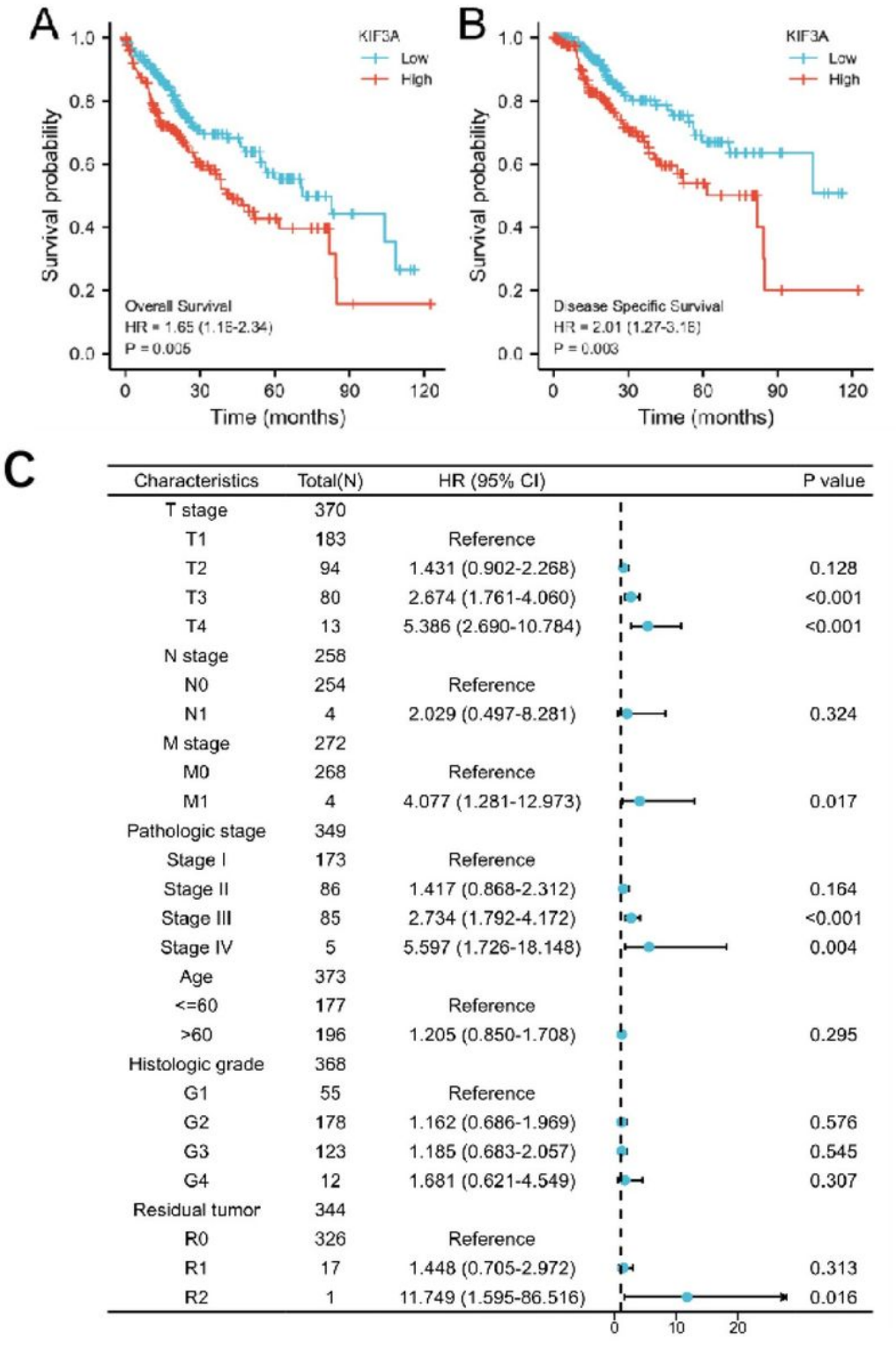

Figure 4

Prognostic values of KIF3A expression in patients undergoing HCC assessed using the Kaplan-Meier method. Overall survival (A) and disease-specific survival (B) in HCC patients having high vs. low KIF3A levels. (C) Forest map on the basis of multivariate Cox analysis for overall survival.

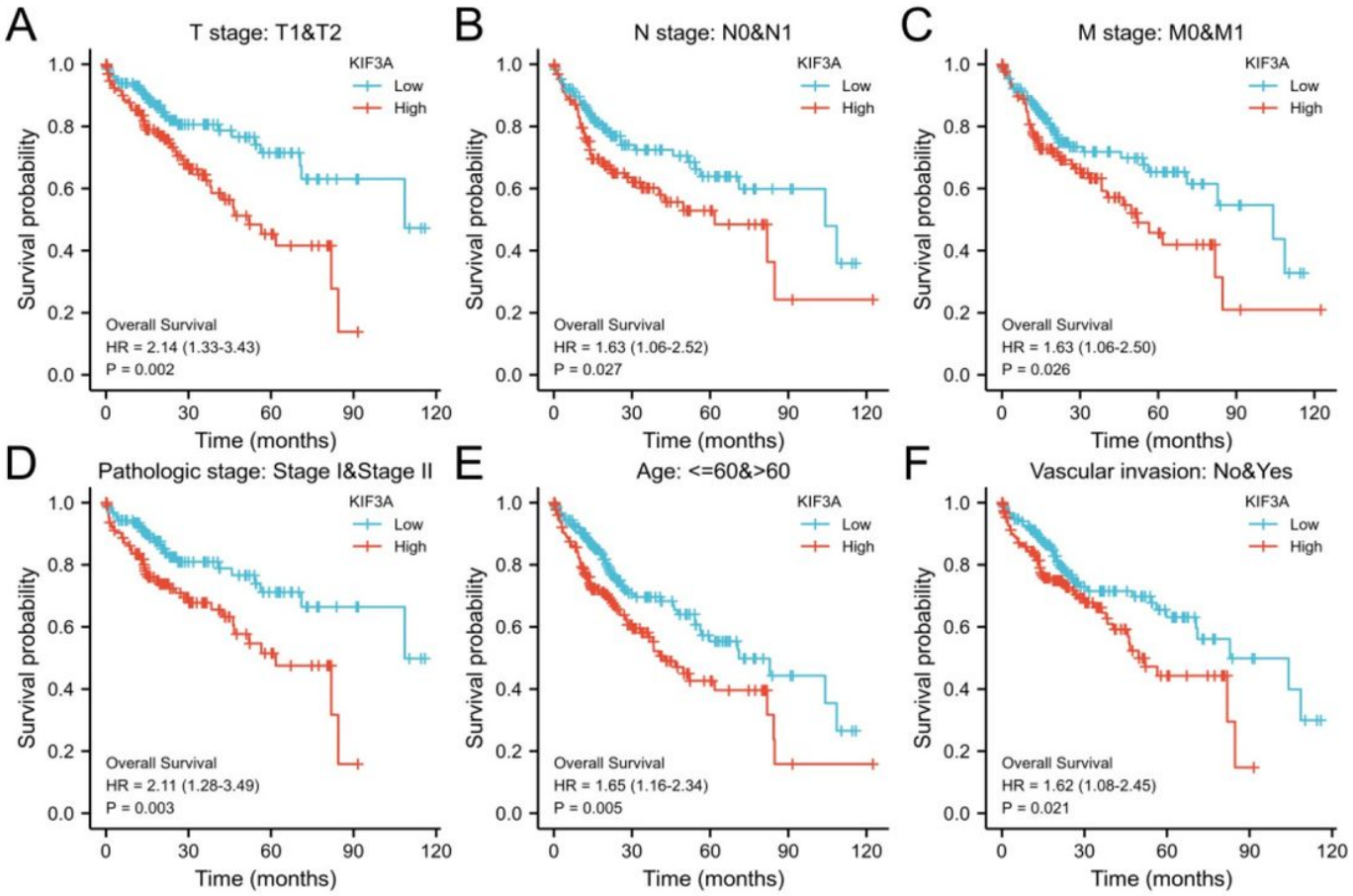

Figure 5

Prognostic values of KIF3A expression in patients suffering from HCC assessed using the Kaplan-Meier method in various subgroups. (A-F) OS survival curves of T1 and T2, N0 and N1, M0 and M1, Pathologic stage I and II, age >60 years, Vascular invasion subgroups between high and low KIF3A patients undergoing HCC.

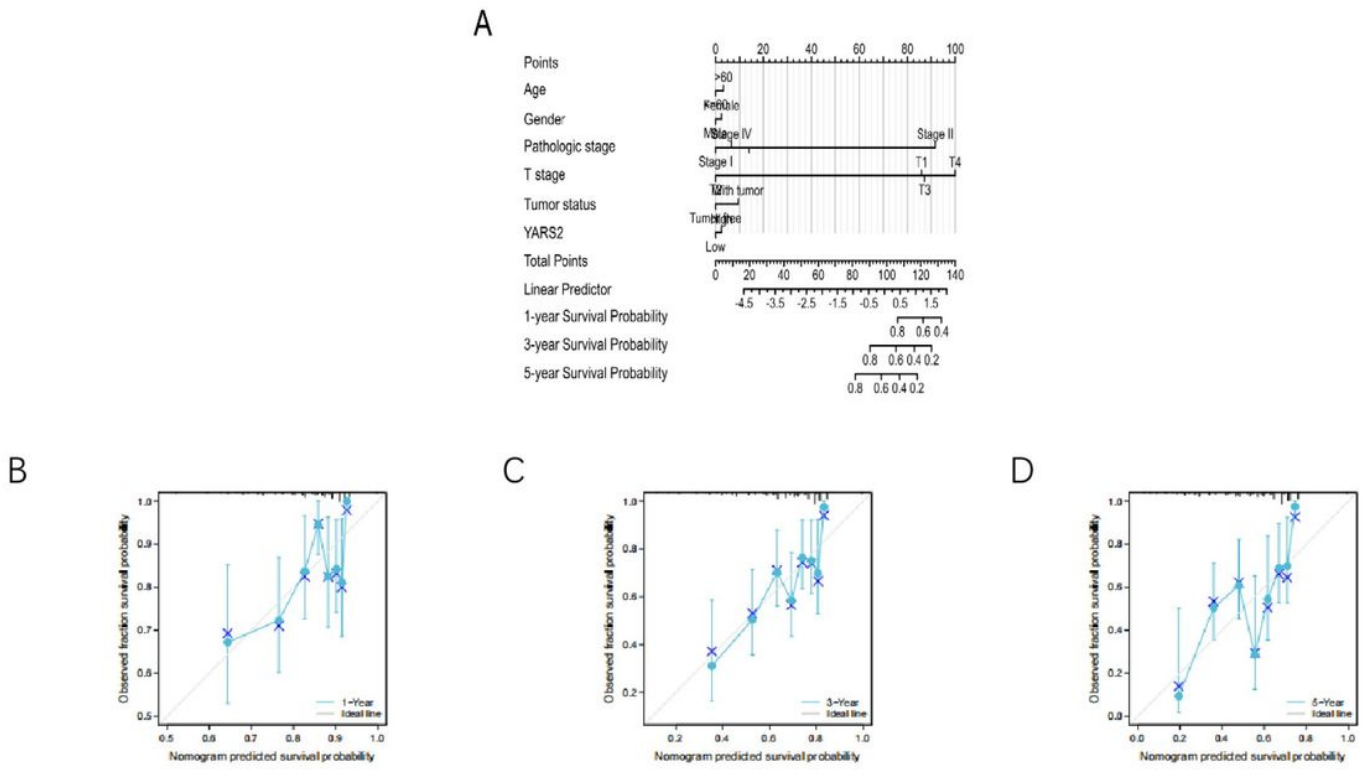

Figure 6

A nomogram and calibration curves for predicting one-, three-, and five-year overall survival rates of patients suffering from HCC. (A) A nomogram for predicting one-, three-, and five-year overall survival rates in HCC patients. (B-D) Nomogram calibration curves for one-, three-, as well as five-year overall survival rates in HCC patients.

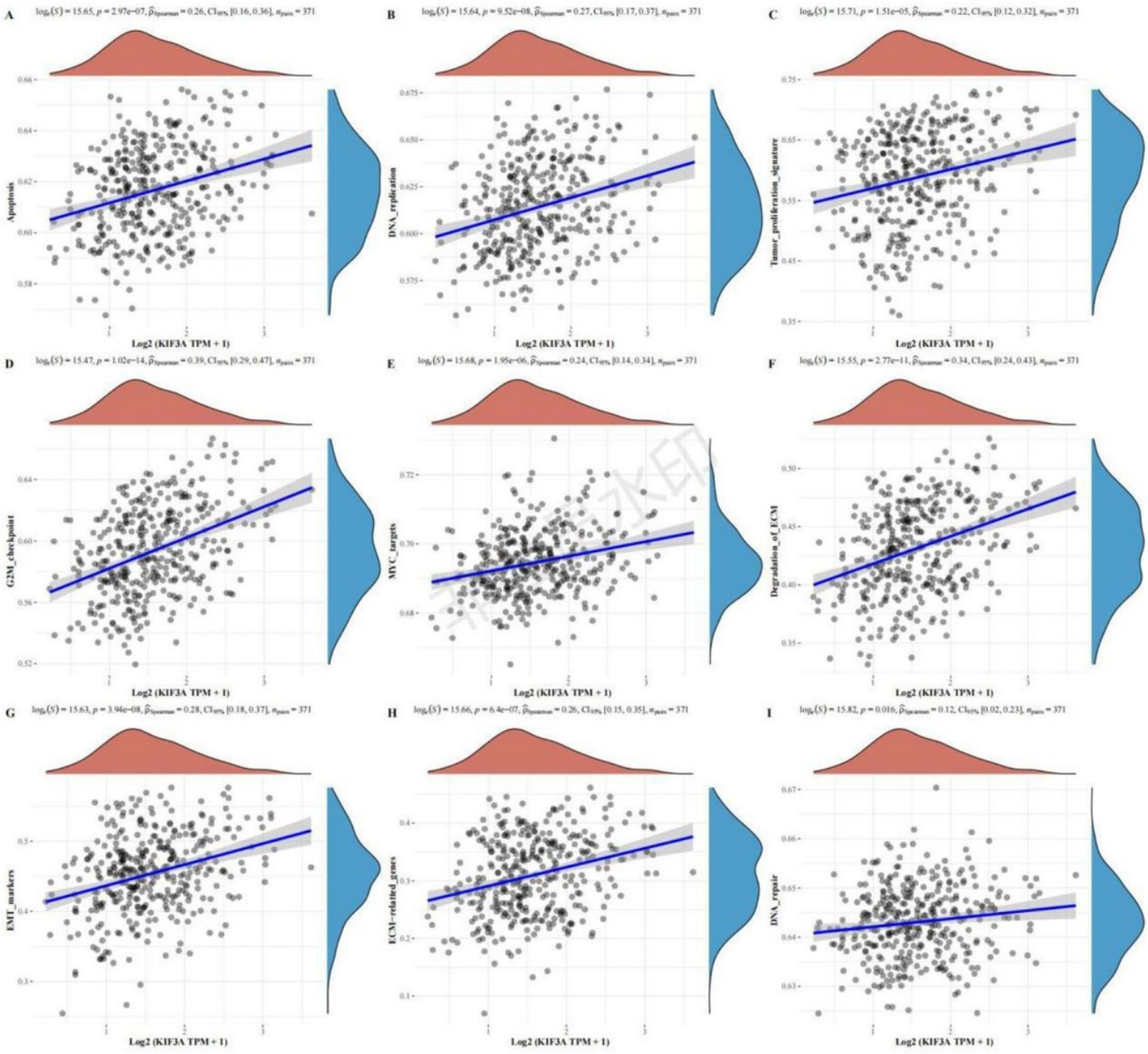

Figure 7

Spearman's correlations were used to examine the relationships between individual genes and pathway scores. Besides, the abscissa stands for gene expression distribution, and the ordinate stands for pathway score distribution. The density curve on the right indicates the distribution trend of pathway immune score, while the upper-density curve stands for the distribution trend of gene expression. In addition, the value at the top stands for the correlation p value, correlation coefficient, as well as the method of calculation for correlation.

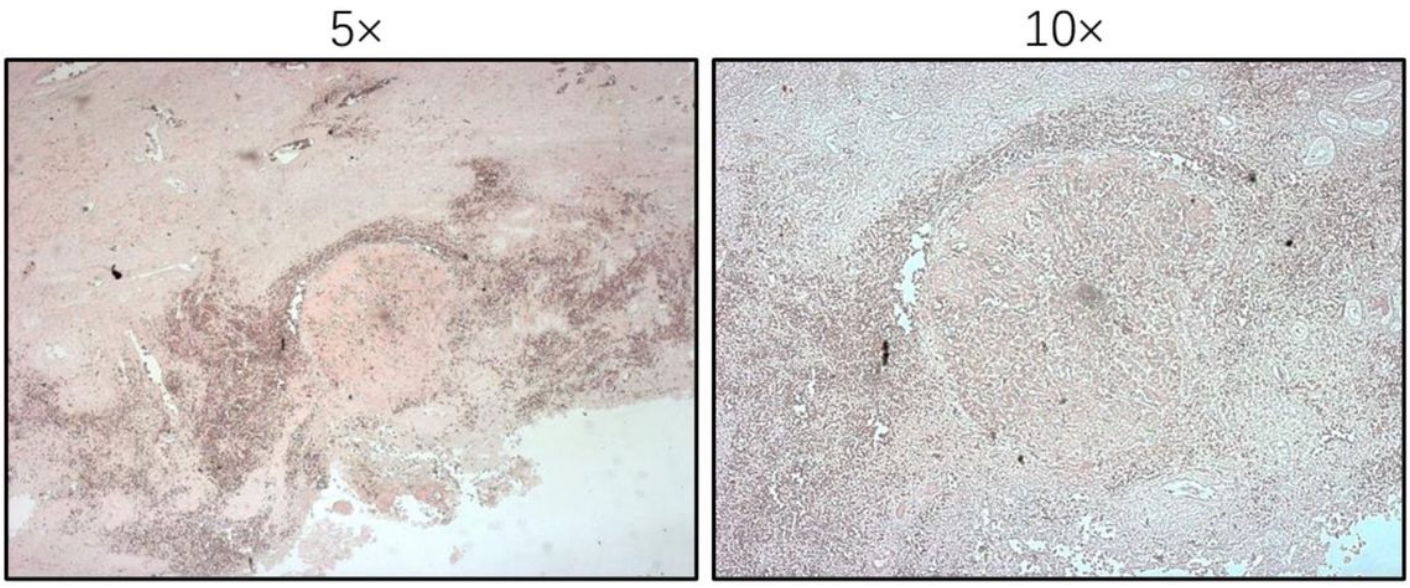

Figure 8

Semi-quantitative analysis of KIF3A expression and staining in HCC(Cancer and adjacent tissues)

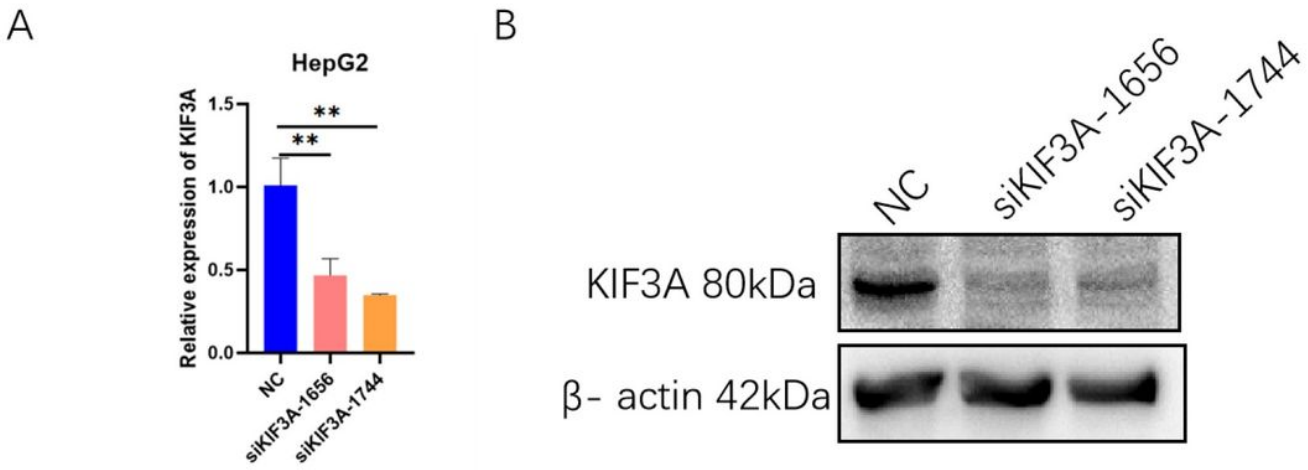

Figure 9

Suppression of HCC cell growth and invasion by KIF3A silencing. KIF3A expression within HCC cells analyzed through qRT-PCR (A) and WB assays (B)

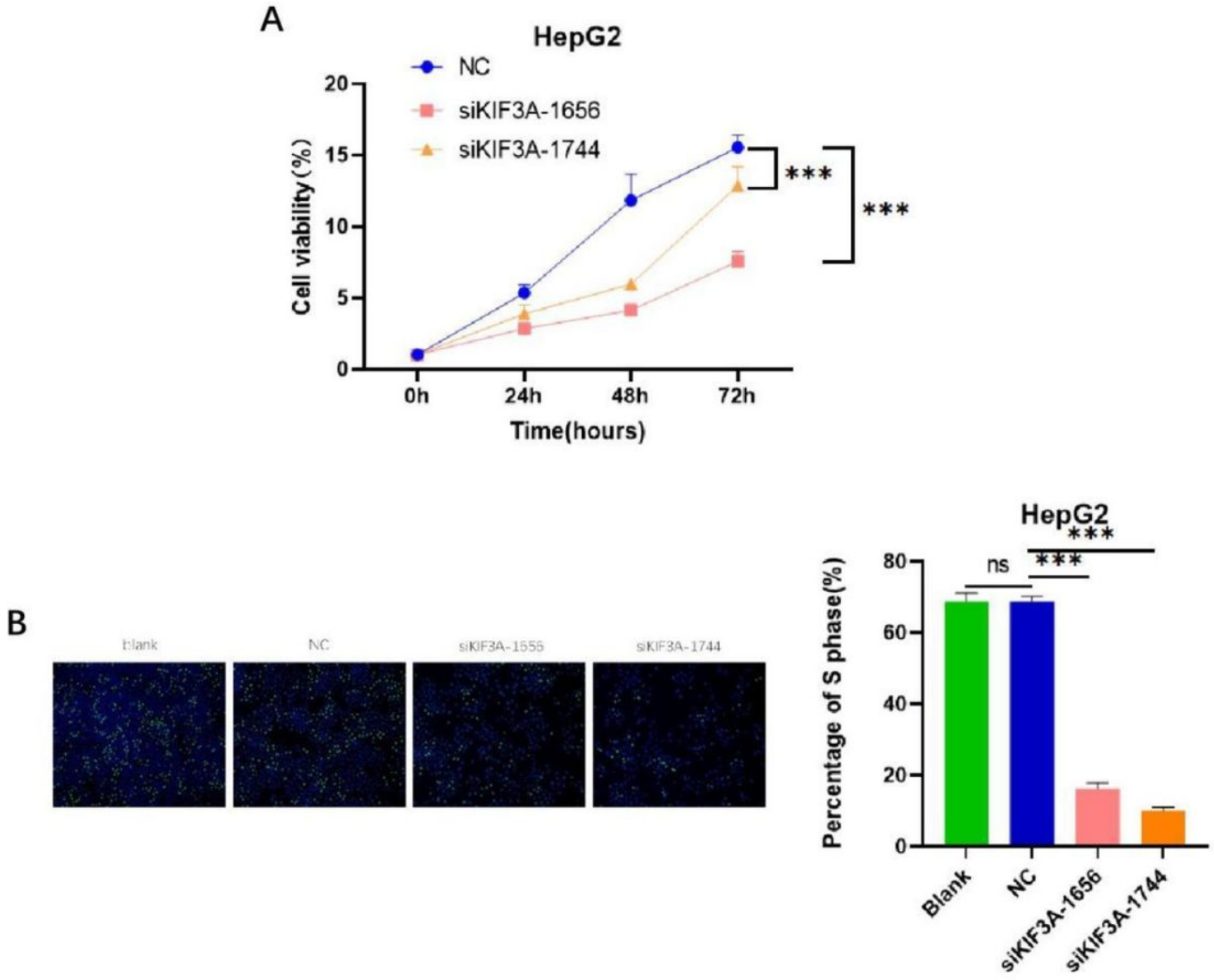

Figure 10

HepG2 cell proliferation analyzed by CCK-8(A) and EDU assays(B). Results are indicated as mean±SD. ***p<0.001.

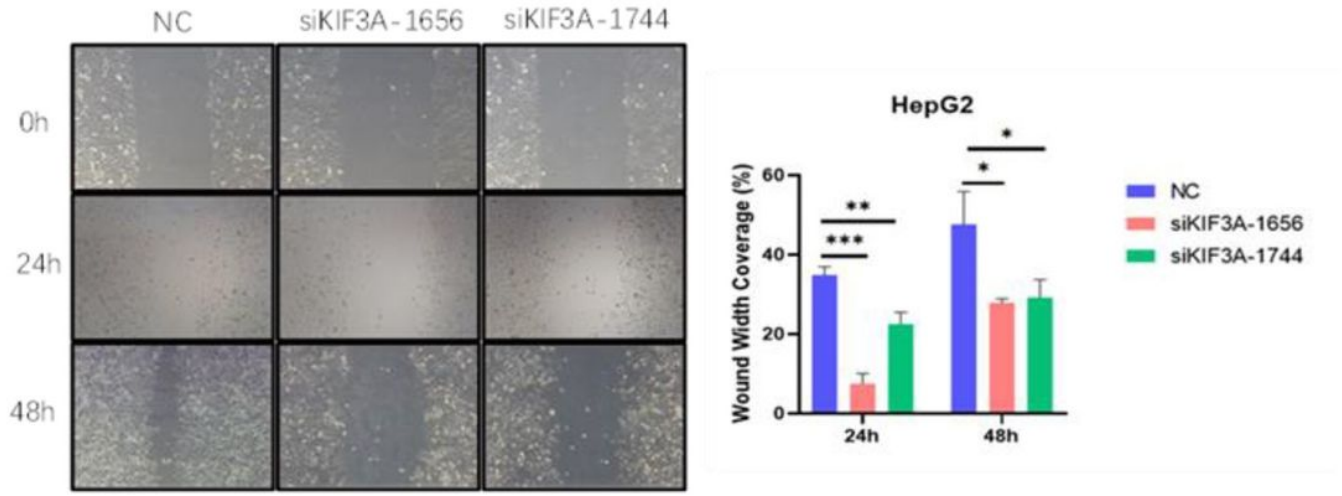

Figure 11

HepG2 cell migration assessed using scratch assay. Results are shown to be mean±SD. ***p<0.001.

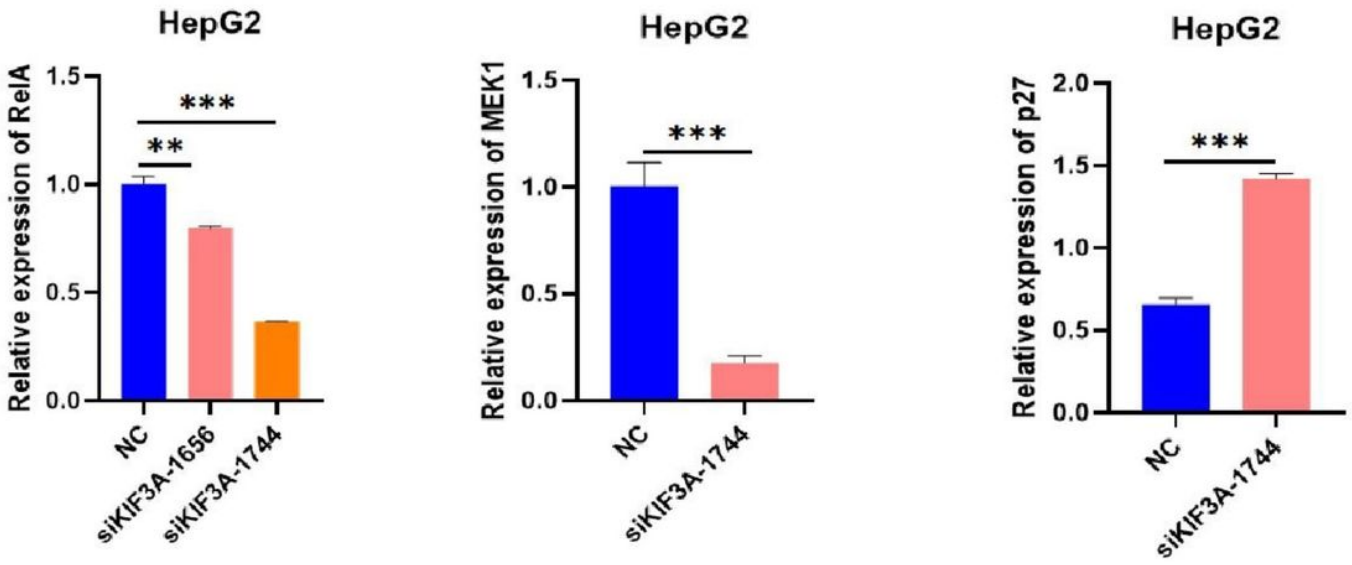

Figure 12

RELA expression analyzed through qRT-PCR following si-KIF3A transfection in HepG2 cells. Results are indicated to be mean±SD. ***p<0.001.

Supplementary Files

This is a list of supplementary files associated with this preprint. Click to download.

- Westernblotsupplementaryfile.rar